FEA for 2D Orthogonal Cutting

Group 5:

Henry Allan-Jones (2162237)

Alexander Dawes (2206650)

Elliott Dyson (2211761)

Freya Harris (2043727)

Adam Lokkerbol (2141143)

Cameron Middleton Morris (2161994)

Outline

- Introduction and Background
- Development of the FE model
- Results and Discussion
- Conclusion

Introduction to 2D Orthogonal Cutting

- Tool piece removes a layer of material from workpiece to form a chip.
- Using FEA shows the effect of parameters on quality of finish and tool wear.
- Quicker and cheaper than physical experiments.

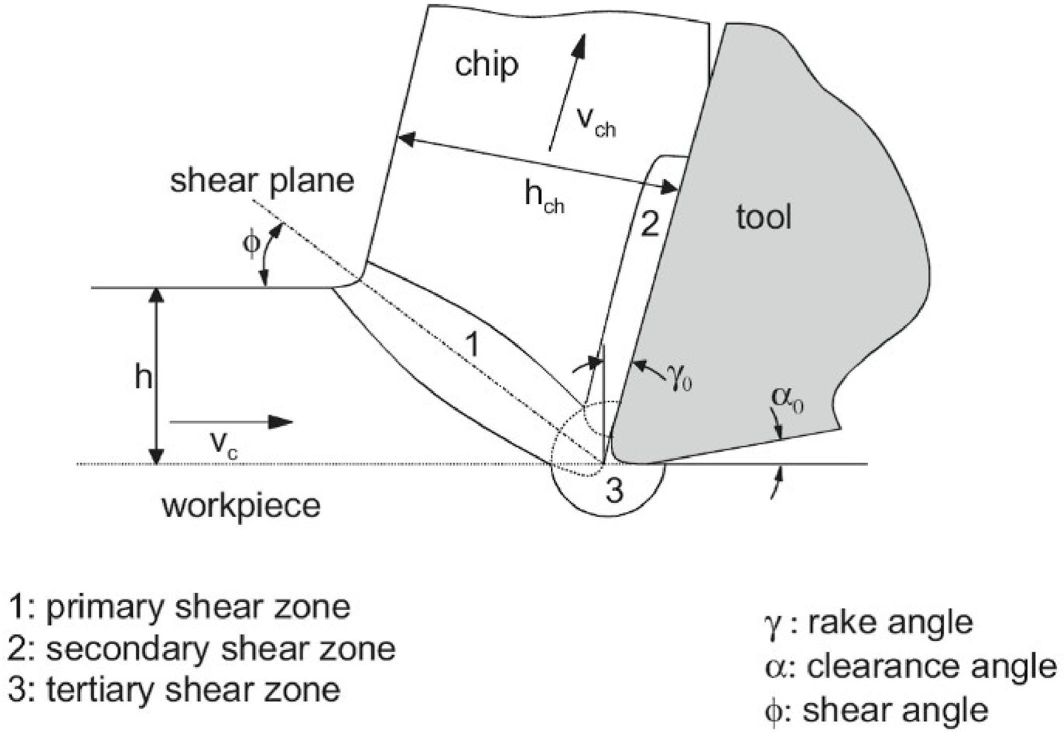

Figure 1: Parameters and deformation zones in orthogonal cutting (Bedzra et al, 2013)

Literature Review

Material and damage models
Thermal properties
Interaction properties
Different meshing methods

Table 1: Literature Review Summary

Aims & Objectives

1. Develop a finite element model to simulate the two-dimensional orthogonal cutting process.
2. Validate our model against an existing paper:

Finite element simulation of two dimensional orthogonal cutting process and comparison with experiments

3. Perform a mesh sensitivity analysis
4. Explore the impact different friction models

Development of the Model
- Validation Paper

Finite element simulation of two dimensional orthogonal cutting process and comparison with experiments Bedzra, R. et al (2013)

Workpiece – IN718 nickel-based alloy

Tool – Tungsten carbide

Material model – Johnson Cook

Mesh Elements – Quadrilateral CPE4RT

Boundary conditions – Fixed at left and bottom

Development of the Model
- Material and Damage models

Johnson-Cook plastic law:

$$\sigma = \left[A + B\overline{\varepsilon_{\mathrm{p}}}^{n}\right] \times \left[1 + C\ln\left(\frac{\dot{\overline{\varepsilon}}_{\mathrm{p}}}{\dot{\overline{\varepsilon}}_{0}}\right)\right] \times \left[1 - \left(\frac{T - T_{\mathrm{ref}}}{T_{\mathrm{melt}} - T_{\mathrm{ref}}}\right)^{m}\right]$$

Johnson-Cook damage model:

$$\overline{\epsilon_f} = \left[D_1 + D_2 e^{(D_3\sigma^*)}\right] \times \left[1 + D_4 \ln\left(\frac{\dot{\overline{\varepsilon}}_p}{\dot{\varepsilon}_0}\right)\right] \times \left[1 + D_5\left(\frac{T - T_{ref}}{T_{melt} - T_{ref}}\right)\right]$$

(Jula et al,, 2012) (Soliman et al., 2020)

Development of the Model
- Part Geometry set up

Tool Geometry – 2d Analytical rigid

Tool Rake angle/°	0
Tool Flank angle/°	10
Tool Radius/m	1.00E-05

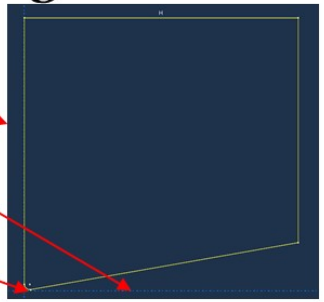

Workpiece Geometry – 2D Deformable rigid

Workpiece length/m	5.00E-03
Workpiece height/m	2.00E-03

Assembly Geometry

Finely meshed region height/m	1.00E-04
Depth of cut/m	5.00E-05

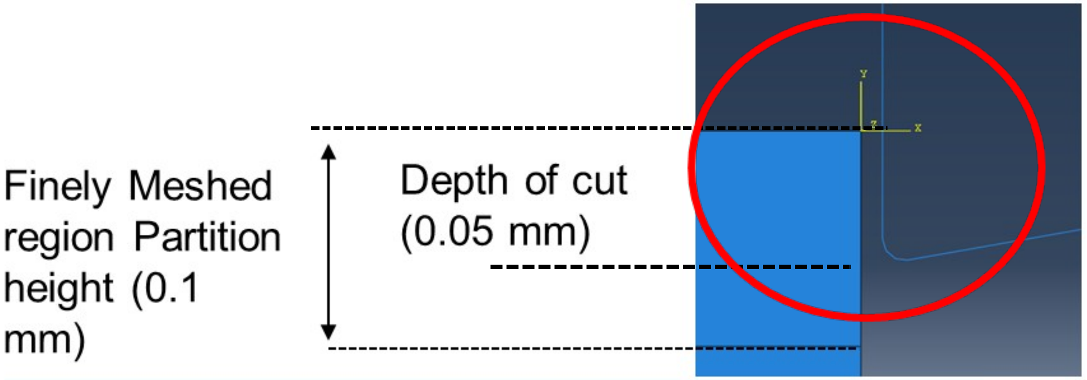

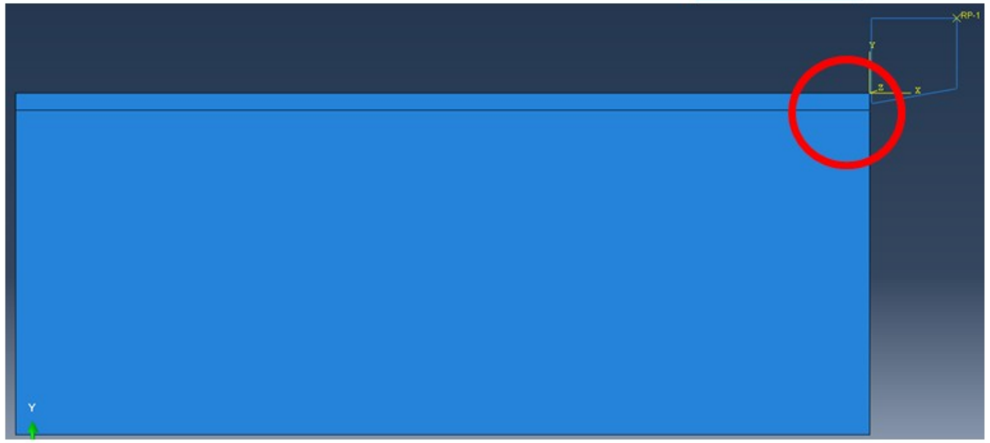

Development of the Model
- Material and Damage models –Workpiece

All Units are SI Base units

Density

	Mass Density
1	8220

Elastic

	Young's Modulus	Poisson's Ratio
1	217000000000	0.3

Plastic - Johnson Cook Hardening

Hardening: Johnson-Cook

Data

	A	B	n	m	Melting Temp	Transition Temp
1	1490000000	904000000	0.777	1.689	1570	293

Rate dependant hardening

Data

	C	Epsilon dot zero
1	15000	0.01

Section - Plane Stress Thickness

Edit Section

Name: workpiece-material

Type: Solid, Homogeneous

Material: IN-718

☑ Plane stress/strain thickness: 0.00035

OK Cancel

0.00035 to account for the workpiece 3D thickness

Damage Johnson Cook Damage Model

Accumulation Power: 1

▼ Suboptior

Data

	d1	d2	d3	d4	d5	Melting Temperature	Transition Temperature	Reference Strain Rate
1	0	2.031	0	0.014	0	1570	293	0.01

Fracture point

Damage Evolution

Type: Energy

Softening: Linear

Degradation: Maximum

Mixed mode behavior: Mode-Independent

Mode mix ratio: Energy

☐ Power

☐ Use temperature-dependent data

Number of field variables: 0

Data

	Fracture Energy
1	3105

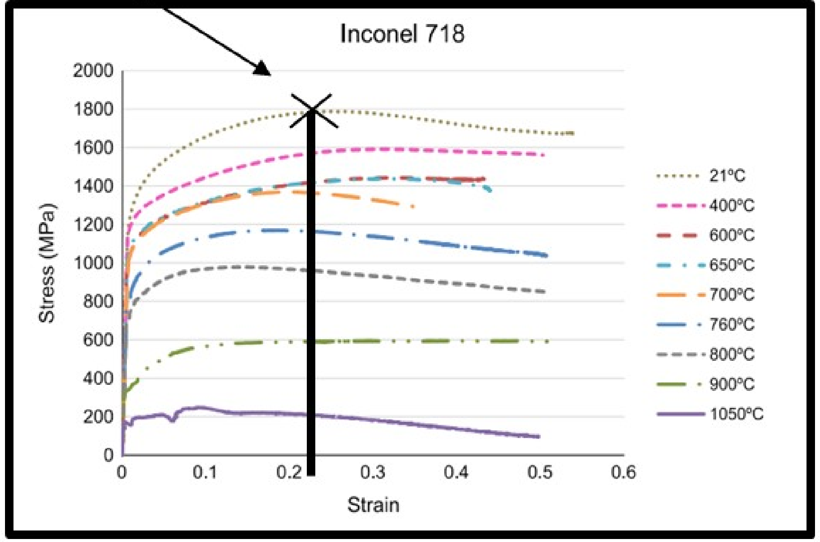

Development of the Model
- Step and Interaction

Step – Dynamic explicit

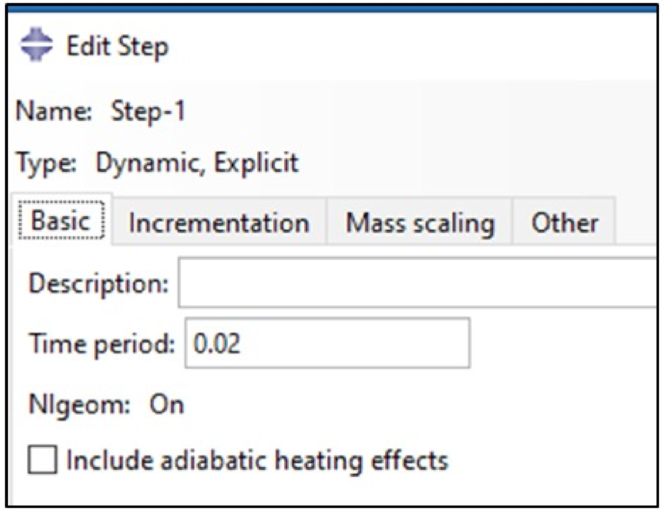

Time period calculated using speed of tool and length of workpiece

Mass Scaling adjusted to improve simulation time during the model development phase

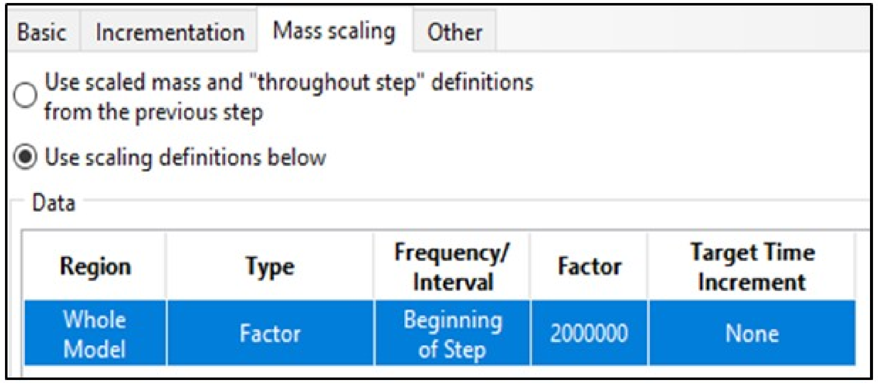

Region	Type	Frequency/ Interval	Factor	Target Time Increment
Whole Model	Factor	Beginning of Step	2000000	None

Surface to surface contact
Defined between tool and workpiece

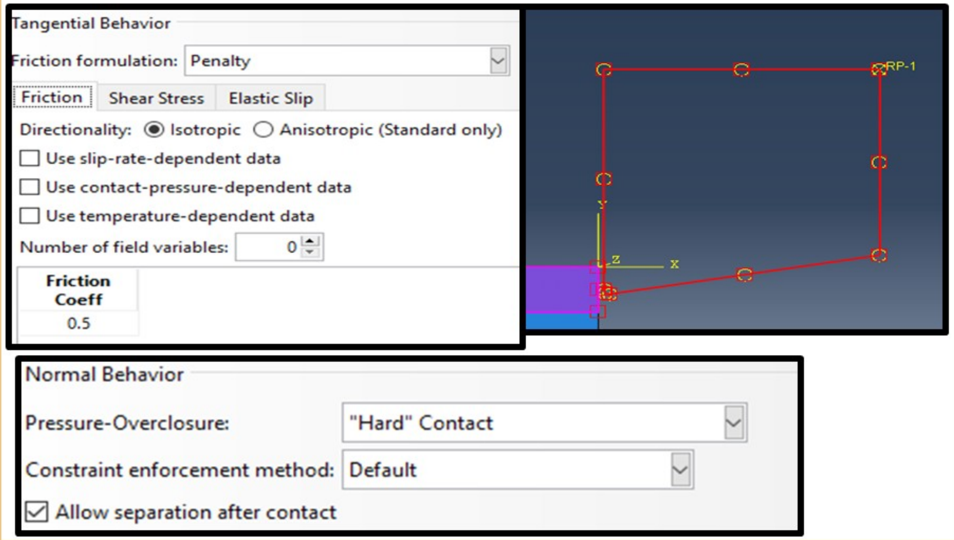

Self-surface contact

Applied to top and side surfaces applied

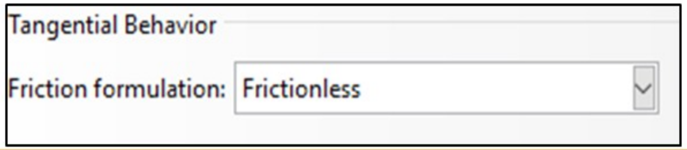

Development of the Model
- Rigid body constraint

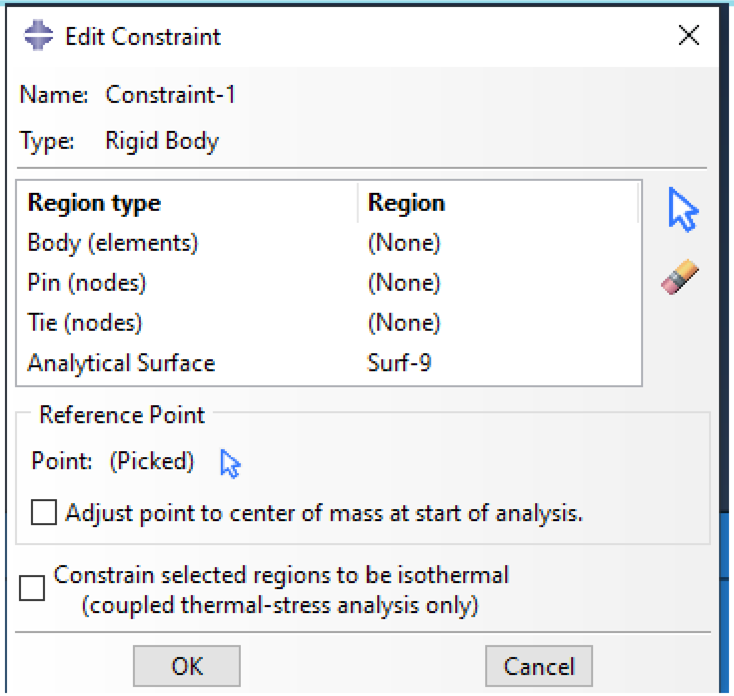

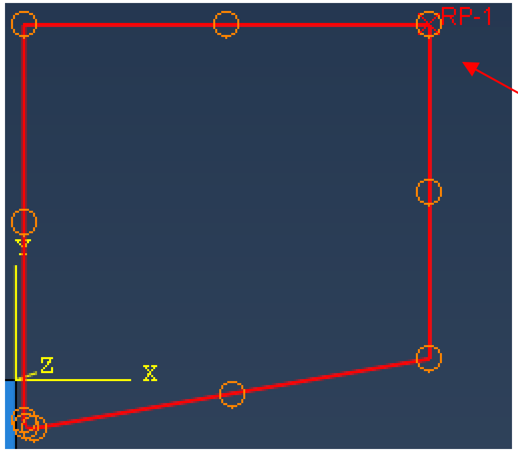

A rigid body constraint was applied between the tool and the reference point

Development of the Model
- Boundary Conditions

Workpiece

Displacement/rotation boundary condition applied to bottom surface, fixed in U1, U2 and UR3

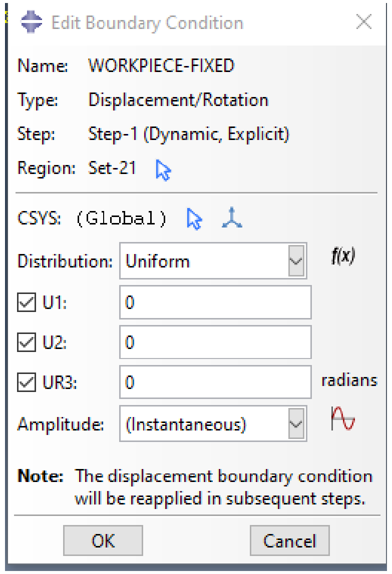

Tool Velocity

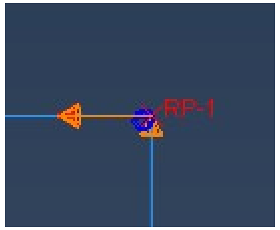

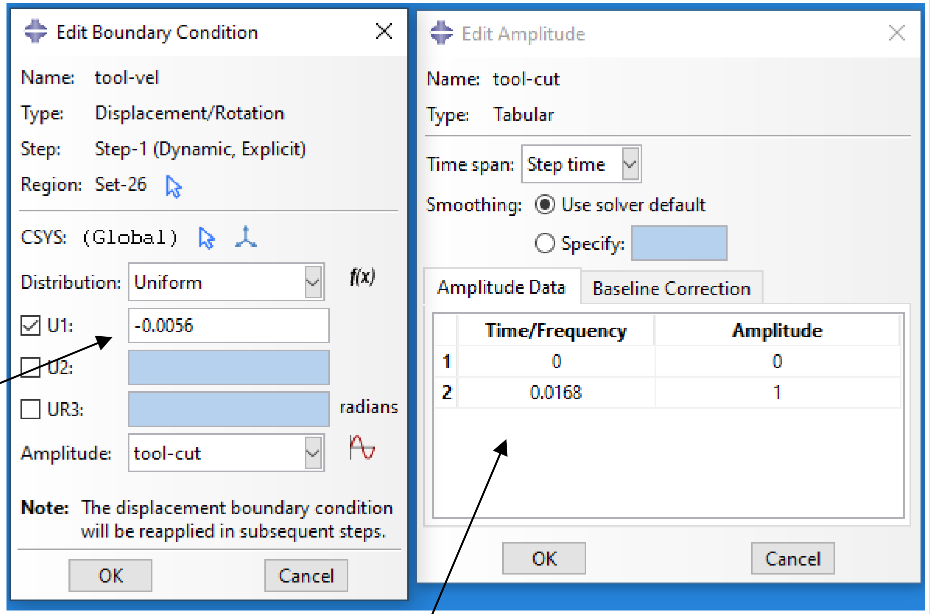

Tool only allowed to move in x-direction

Tabular amplitude defined

Development of the Model - Meshing

- ALE was chosen as it can handle the required levels of distortion, it is also the most used in literature for 2D orthogonal cutting.

- There are two parts per ALE step, the mesh-sweep and the advection sweep.

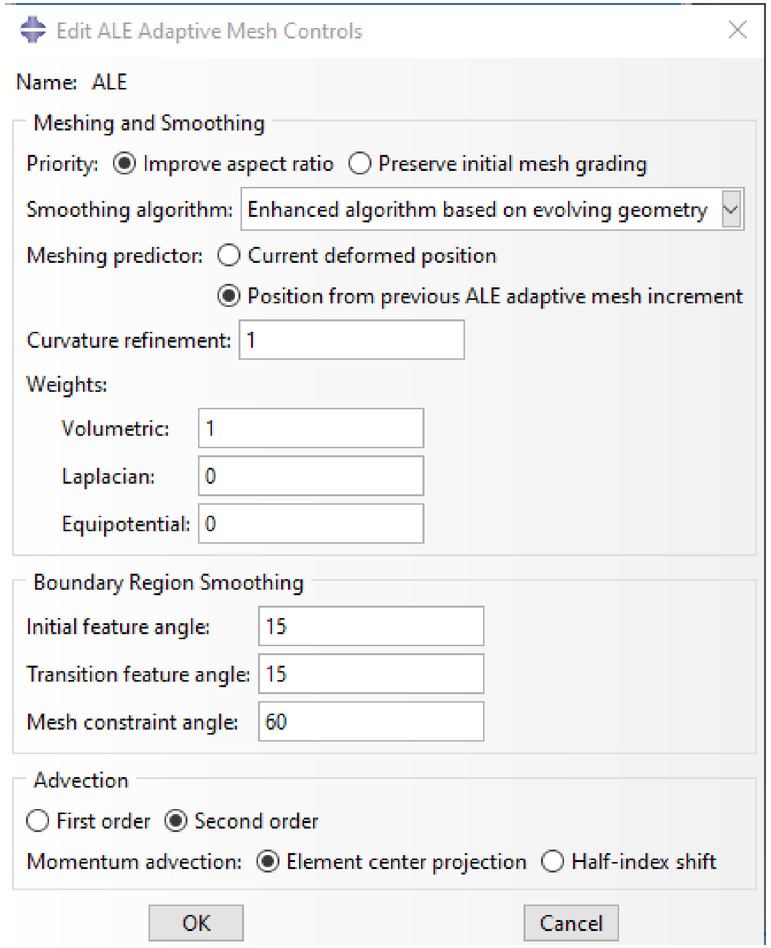

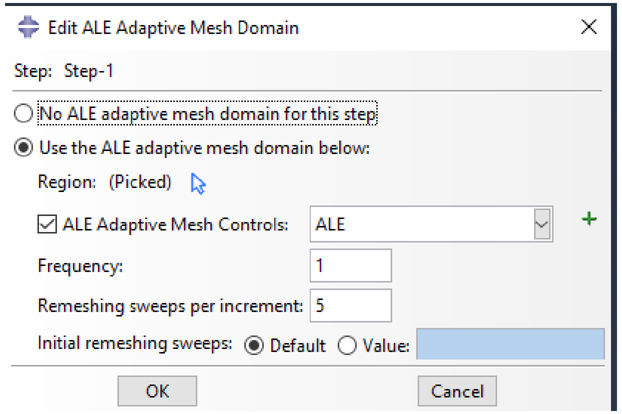

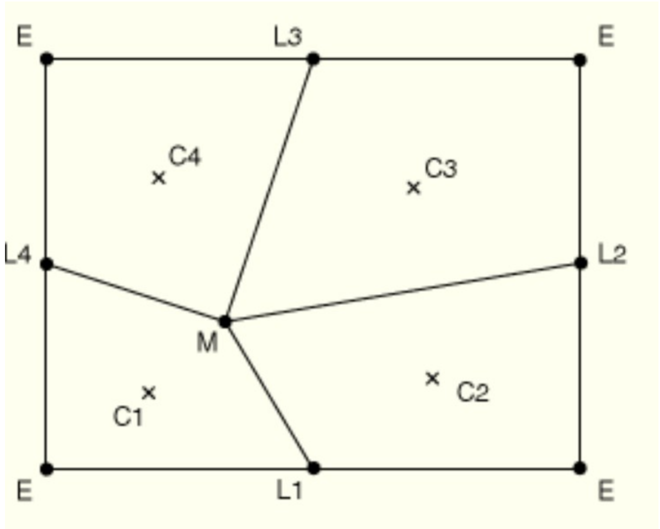

Development of the Model - Meshing: Workpiece

- Chosen Element Type: Fine section – CPS4R, Lower Section: Structured Quadrilateral

- Use of ‘seed edge bias’: Element size gradient – Increased efficiency

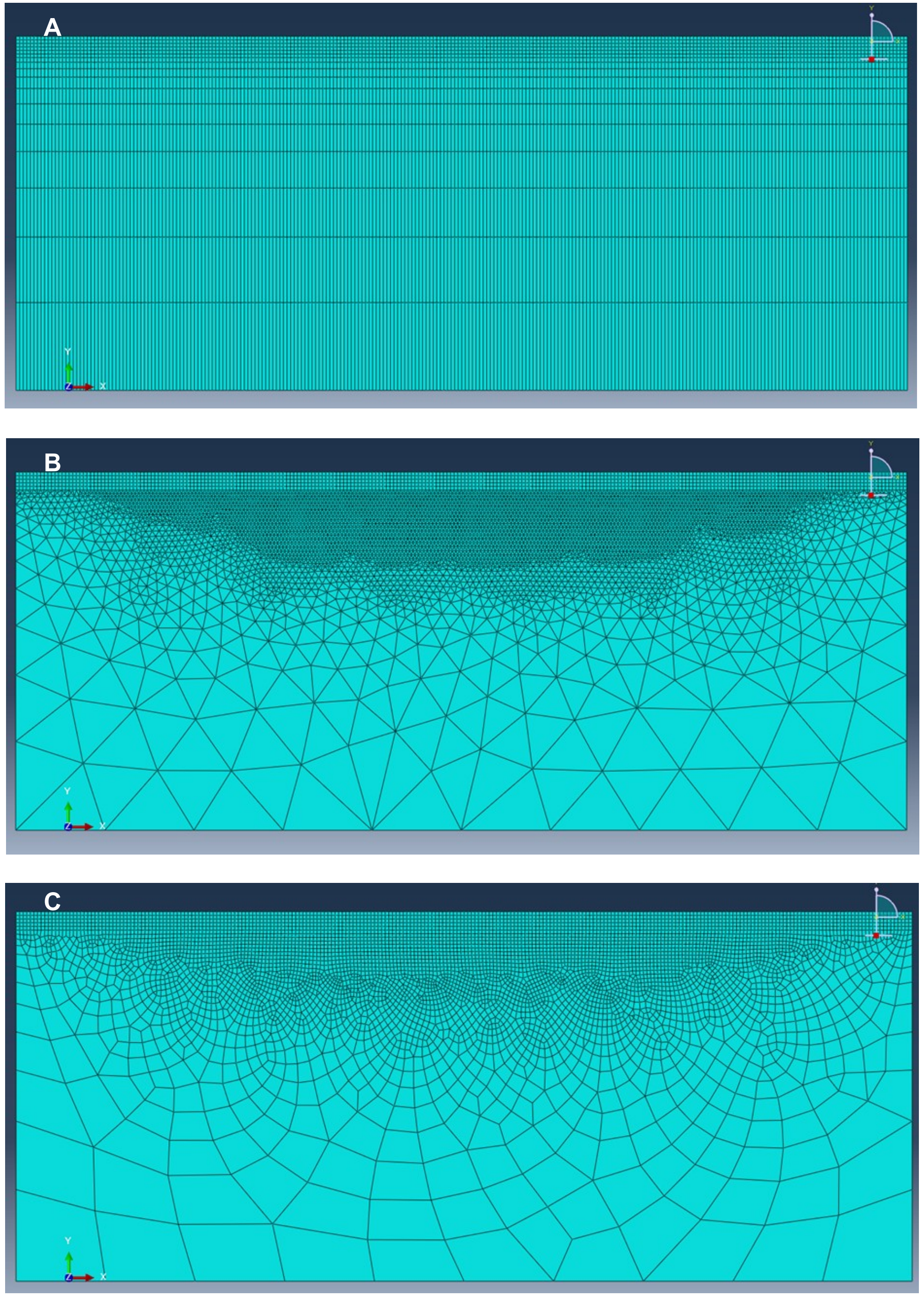

Figure 1A: Swept Quadrilateral
Figure 1B: Structured Triangular
Figure 1C: Structured Quadrilateral

Results and Discussion
- Mesh Sensitivity Analysis

- The average cutting force was calculated for each element size.
- The **1.5E-05 m** mesh was chosen since it was closest to the experimental average cutting force of **234 N** – with an **11%** error.
- The **1E-05 m** mesh was equally accurate but computationally more expensive

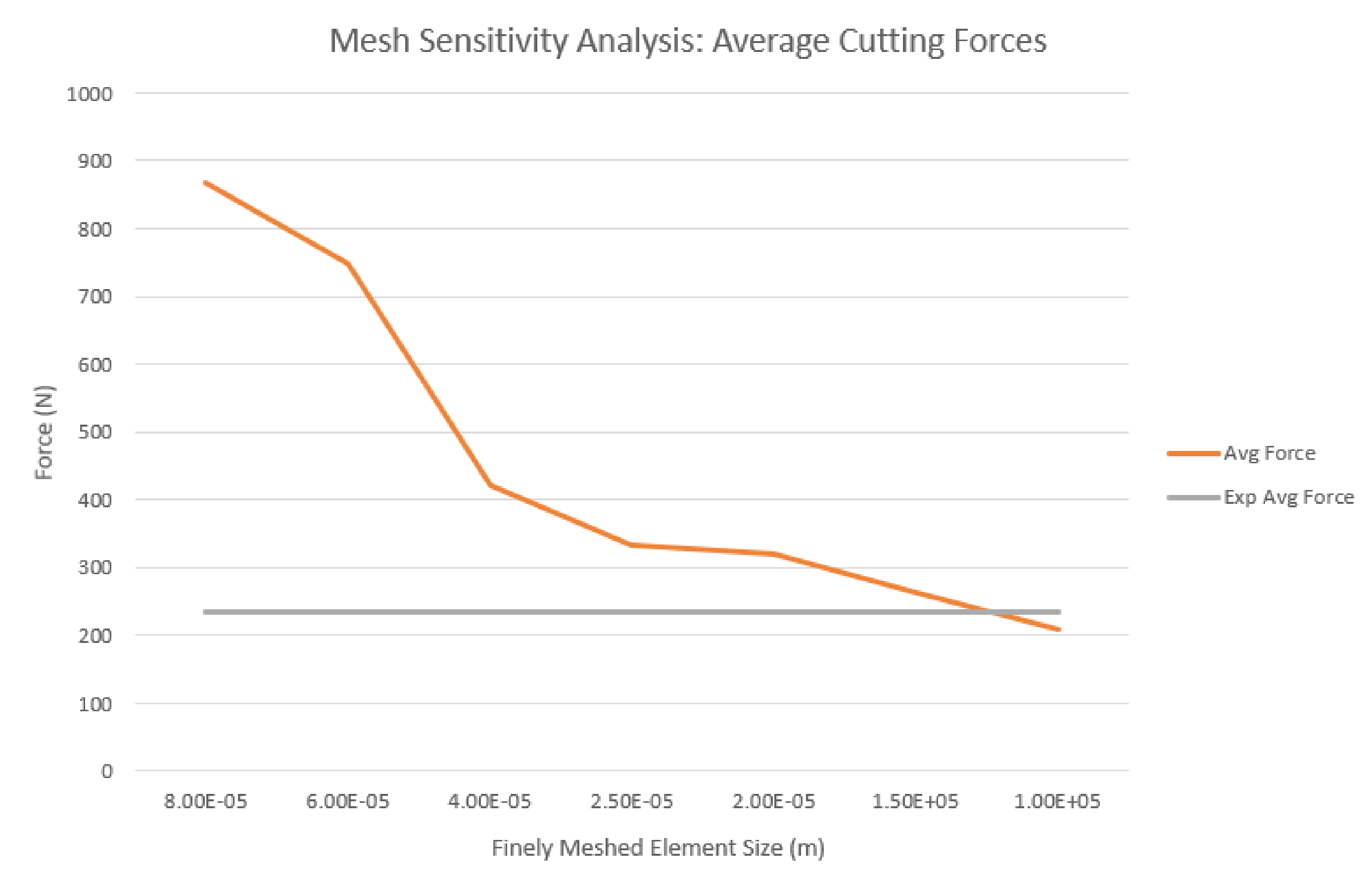

Figure 1: Average Cutting Force Graph

Results and Discussion
-Validation via Chip Formation

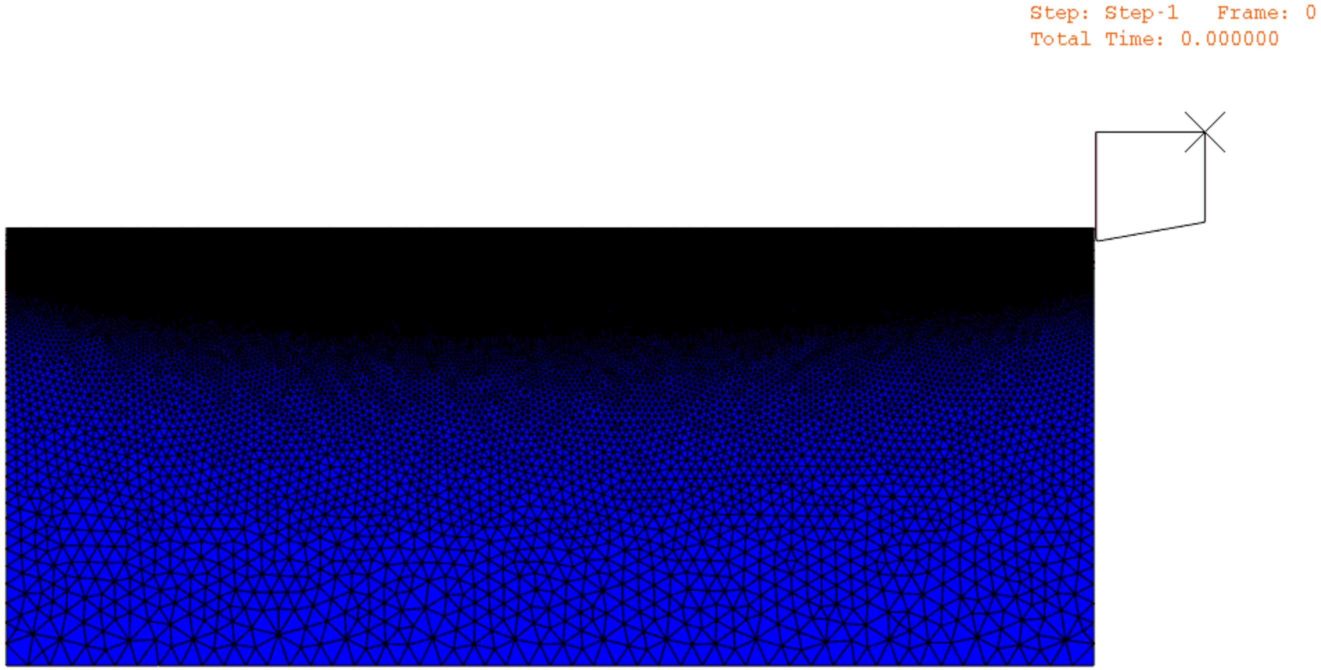

Figure 1 – Video of chip formation

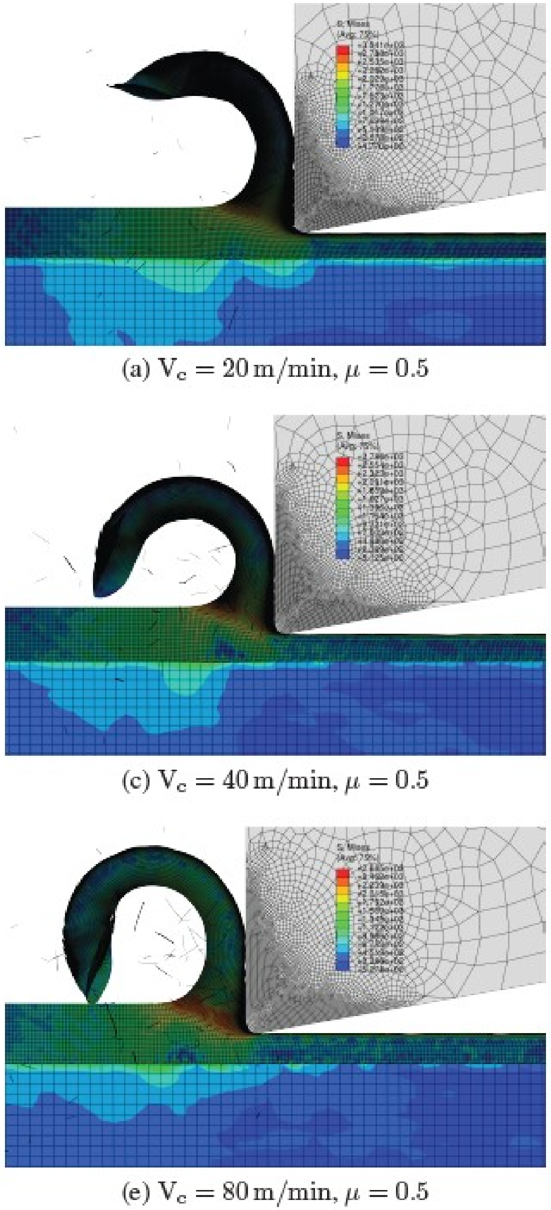

Figure 2 – Chip formation for different cutting speeds
Bedzra, R. et al (2013)

Mass Scaling Effects

- A mass scale factor of **2E+06** was used for the simulation.
- The kinetic energy peaked at **9.86%** of the total internal energy.
- This is less than the **10%** rule of thumb.

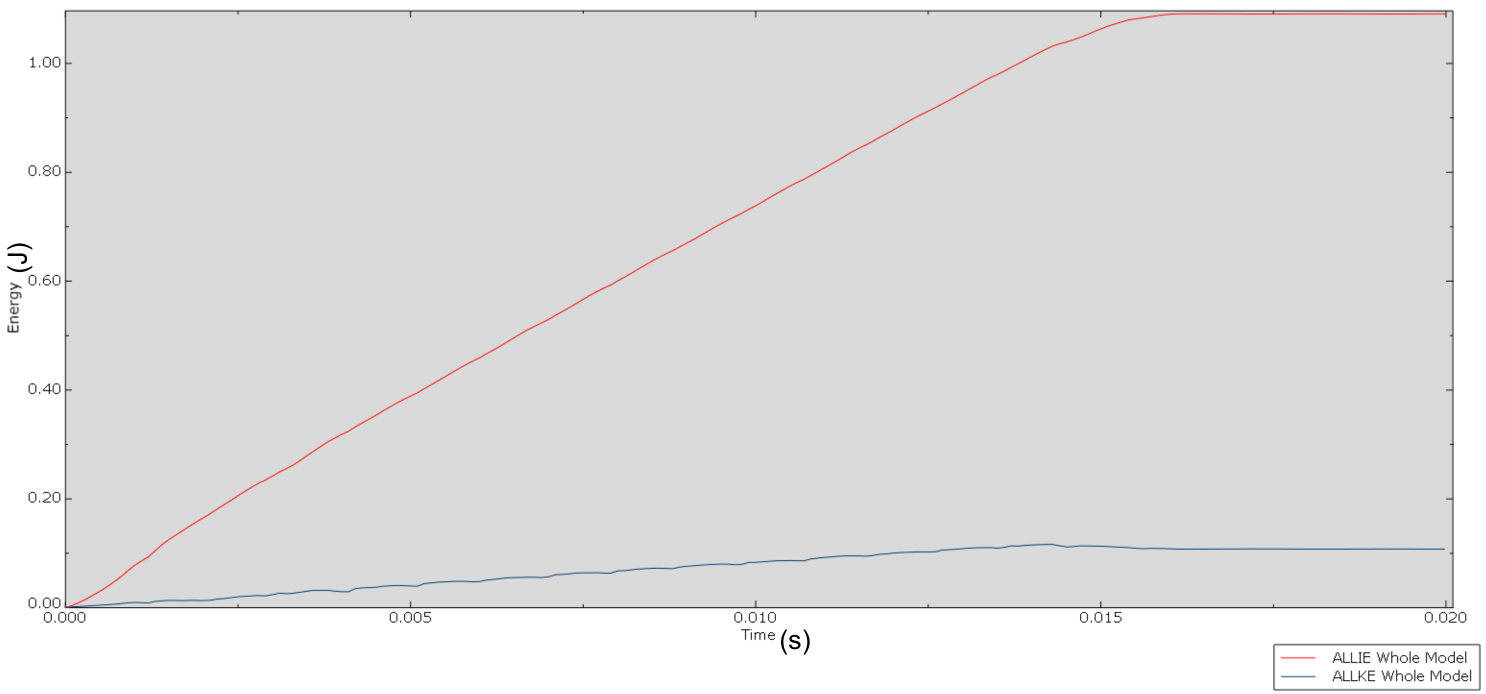

Figure 1: Internal and Kinetic Energies

Temperature Results additional steps -Meshing: Tool

- Tool must be meshed to account for thermal interaction

- Finley seeded closer to the tip to preserve the radius feature geometry and enhance thermal solution accuracy at the interaction interface

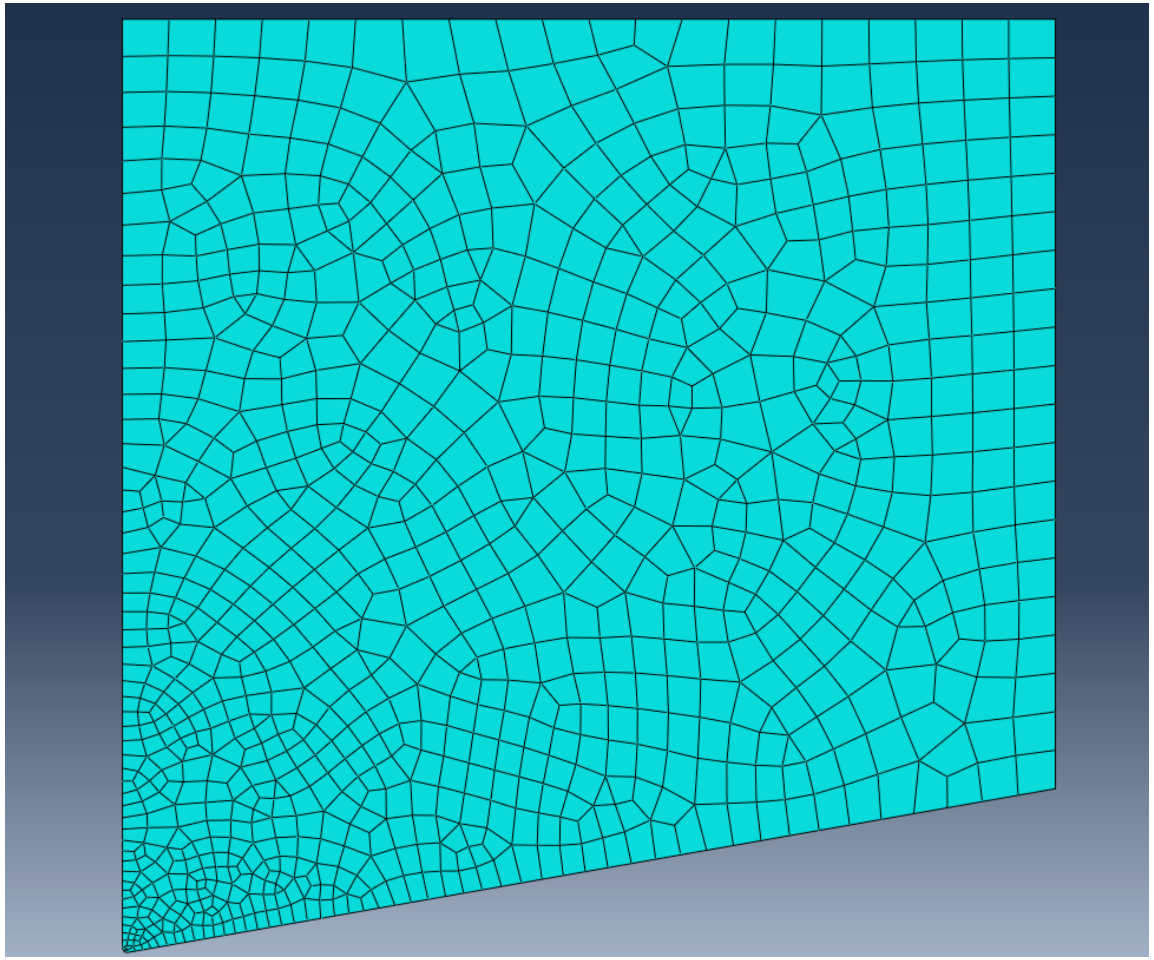

Figure 1: Tool Mesh

Further Development of the Model - Thermal setup

Thermal properties included for tool and workpiece in material section (Thermal conductivity, specific heat capacity)

Heat generation as part of the penalty contact interaction property for the tool and workpiece contact

- Element type needs to be specified for both tool and workpiece as coupled-temperature displacement
- The base temperature of the material and workpiece taken as 23 degrees Celsius

Thermal Assumptions used in simulation:

- Workpiece on workpiece contact does not generate heat
- The tool is a rigid body
- Convection and radiation not included

Results and Discussion
- Average Cutting Force for different frictional models

- Meshed tool model obtained Average Cutting Force of **225.09 N** when friction is included as Coulomb friction law (μ=0.5) @ Cutting speed of 40m/min
- **100.3 N** Average force for no friction,(μ=0) hence frictionless interaction is not suitable.
- **234 N** average cutting force from experimental results
- Paper simulation results of **259.83 N** average cutting force

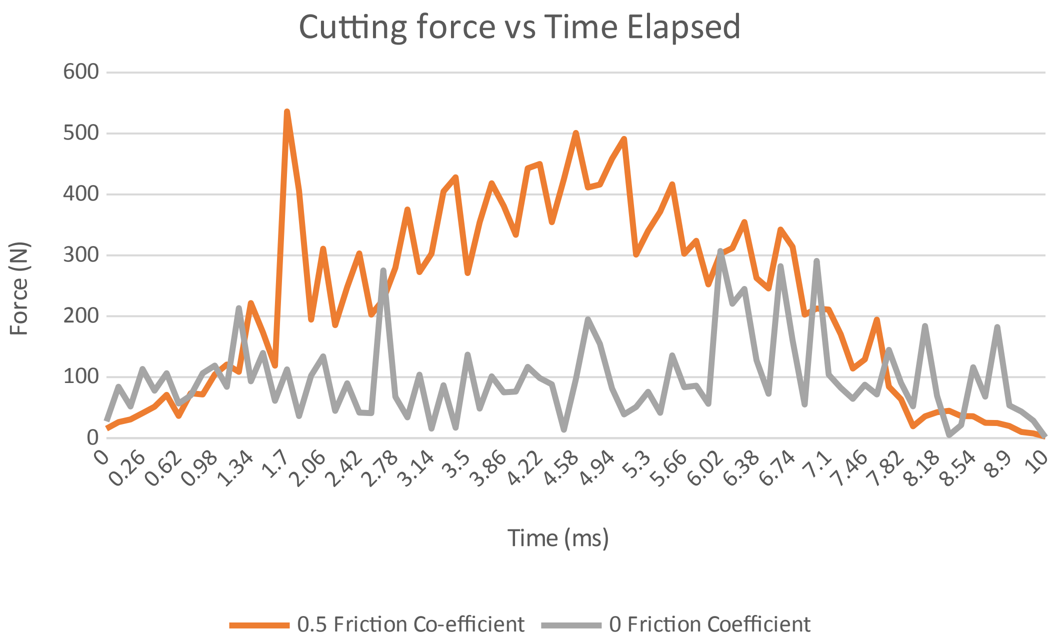

Figure 1: Comparison of tool forces: with and without friction

Results and Discussion - Temperature

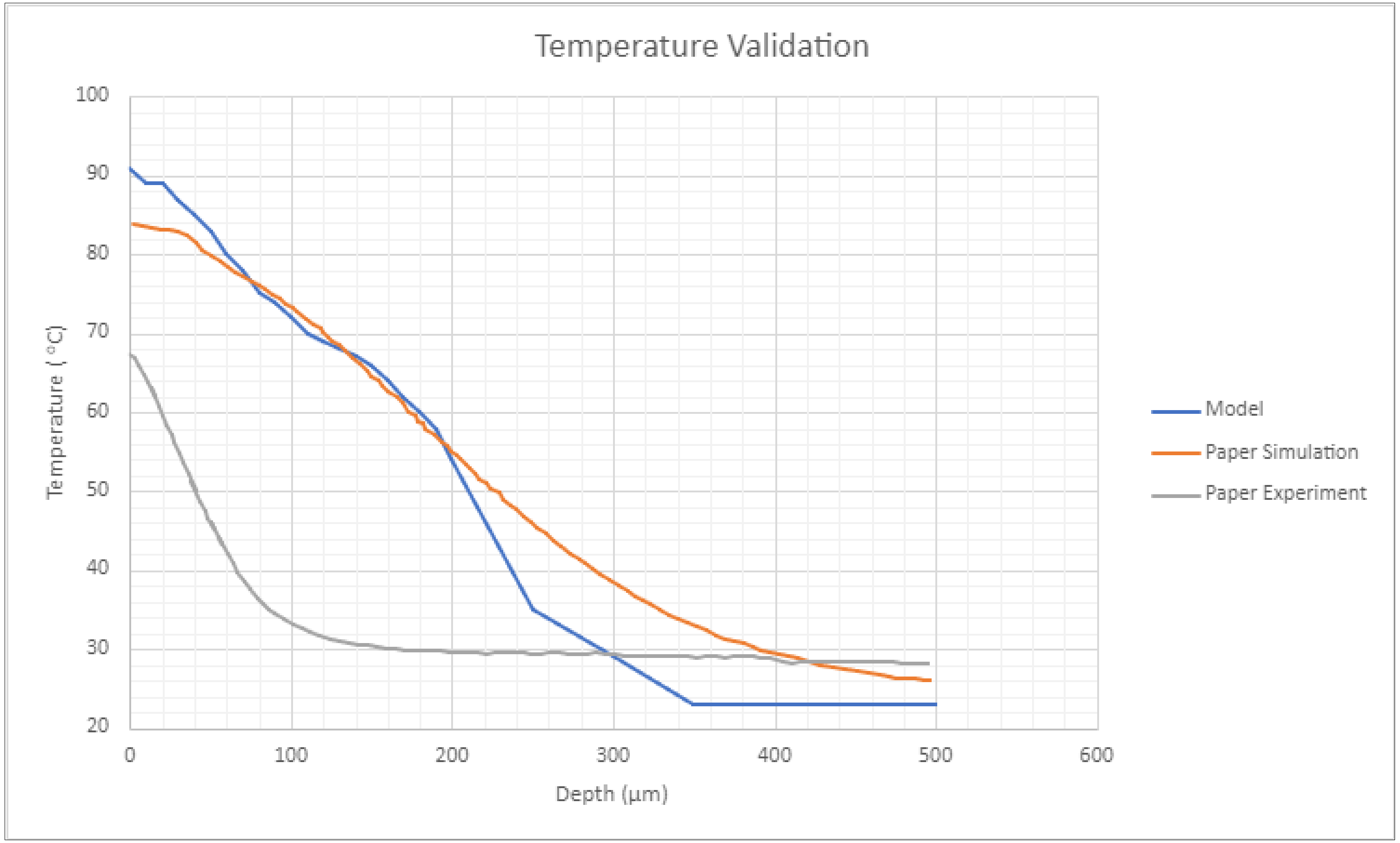

Figure 1: Variation of Temperature with Depth

- Temperature against depth of workpiece, up to **500 µm**, **3.5 mm** behind tool edge at the end of the simulation.
- Maximum within **9%** of peak temperature from simulation results
- Variation, since convection and radiation loses not included in simulations, visible as lower starting temperature and sharper decrease to ambient temperature in the experimental data plot.

Conclusions

- Validated model via cutting force, temperature and chip formation
- The mesh element of size **1.5E-05 m** provided the closest average cutting force to the experimental value – with an error of **11%**.
- Temperature maximum error of **9%**
- Coulomb Friction co-efficient of **0.5** provides more accurate cutting force than frictionless interaction

References

1. Bedzra, R. (2013) 'Finite Element Simulation of Two Dimensional Orthogonal Cutting process and Comparison with Experiments'. *Institut of Applied Mechanics RWTH Aachen and Department of Aerospace Engineering, FH Aachen.*
2. Jula, F.C., Galle, T., De Waele, W. & Borzan, M. (2012). 'FEA modeling of orthogonal cutting of steel: a review'. *International Journal Sustainable Construction & Design.* 3(2) p. 98-105
3. Soliman, H.A., Shash, A.Y., El-Hossainy T.M., Abd-Rabou, M. (2020). 'Cutting Forces and Crater Wear Prediction in Orthogonal Cutting Using Two Approaches of Finite Element Modeling. *Engineering Reports.* 2:e12240
4. Aich, Z., Haddouche, K., Djellouli, K., & Ghezal, A. (2023). An improved thermomechanical modeling for orthogonal cutting of AISI 1045 steel. Results in Engineering, 17, 100789. https://doi.org/10.1016/J.RINENG.2022.100789
5. Bil, H., Kiliç, S. E., & Tekkaya, A. E. (2004). A comparison of orthogonal cutting data from experiments with three different finite element models. International Journal of Machine Tools and Manufacture, 44(9). https://doi.org/10.1016/j.ijmachtools.2004.01.016
6. Ceretti, E., Fallböhmer, P., Wu, W. T., & Altan, T. (1996). Application of 2D FEM to chip formation in orthogonal cutting. Journal of Materials Processing Technology, 59(1-2 SPEC. ISS.). https://doi.org/10.1016/0924-0136(96)02296-0
7. Duan, C. Z., Dou, T., Cai, Y. J., & Li, Y. Y. (2011). Finite Element Simulation and Experiment of Chip Formation Process during High Speed Machining of AISI 1045 Hardened Steel. In AMAE Int. J. on Production and Industrial Engineering (Vol. 02, Issue 01).
8. Gallos, I., Devall, A., Martin, J., Middleton, L., Beeson, L., Galadanci, H., Alwy Al-beity, F., Qureshi, Z., Hofmeyr, G. J., Moran, N., Fawcus, S., Sheikh, L., Gwako, G., Osoti, A., Aswat, A., Mammoliti, K.-M., Sindhu, K. N., Podesek, M., Horne, I., … Coomarasamy, A. (2023). Randomized Trial of Early Detection and Treatment of Postpartum Hemorrhage. New England Journal of Medicine, 389(1), 11–21. https://doi.org/10.1056/NEJMoa2303966
9. Jadhav, A. A., & Ramgir, M. S. (2015). Finite Element Simulation of Orthogonal Cutting Process for Steel Atul Ananda Jadhav. www.ijert.org
10. Klocke, F., Raedt, H. W., & Hoppe, S. (2001). 2D-FEM simulation of the orthogonal high speed cutting process. Machining Science and Technology, 5(3), 323–340. https://doi.org/10.1081/MST-100108618
11. Li, H., Qin, X., He, G., Jin, Y., Sun, D., & Price, M. (2016). Investigation of chip formation and fracture toughness in orthogonal cutting of UD-CFRP. International Journal of Advanced Manufacturing Technology, 82(5–8), 1079–1088. https://doi.org/10.1007/s00170-015-7471-x
12. Merchant, M. E. (1945a). Mechanics of the metal cutting process. II. Plasticity conditions in orthogonal cutting. Journal of Applied Physics, 16(6), 318–324. https://doi.org/10.1063/1.1707596
13. Merchant, M. E. (1945b). Mechanics of the Metal Cutting Process. I. Orthogonal Cutting and a Type 2 Chip. Journal of Applied Physics, 16(5), 267–275. https://doi.org/10.1063/1.1707586
14. Miller, L. (2020). A Thermal-Mechanical Finite Element Analysis of Orthogonal A Thermal-Mechanical Finite Element Analysis of Orthogonal Cutting for Normalized Steels Cutting for Normalized Steels. https://opencommons.uconn.edu/gs_theses/1485
15. Steden, J., & Thimm, B. (2021). A Comprehensive Sensitivity Analysis of Johnson-Cook Plasticity Parameters on Orthogonal Cutting Simulations. Procedia CIRP, 102, 423–428. https://doi.org/10.1016/J.PROCIR.2021.09.072
16. Vasu, C., Thaware, A., Tiwari, G., & Dumpala, R. (2021). Experimental and numerical analysis of orthogonal cutting of high strength aluminium alloy Al7075-T6. IOP Conference Series: Materials Science and Engineering, 1185(1), 012010. https://doi.org/10.1088/1757-899x/1185/1/012010
17. Yaich, M., Ayed, Y., Bouaziz, Z., & Germain, G. (2017). Numerical analysis of constitutive coefficients effects on FE simulation of the 2D orthogonal cutting process: application to the Ti6Al4V. International Journal of Advanced Manufacturing Technology, 93(1–4), 283–303. https://doi.org/10.1007/s00170-016-8934-4
18. Zhang, D., Zhang, X. M., & Ding, H. (2016). A Study on the Orthogonal Cutting Mechanism Based on Experimental Determined Displacement and Temperature Fields. Procedia CIRP, 46, 35–38. https://doi.org/10.1016/J.PROCIR.2016.03.176

Questions